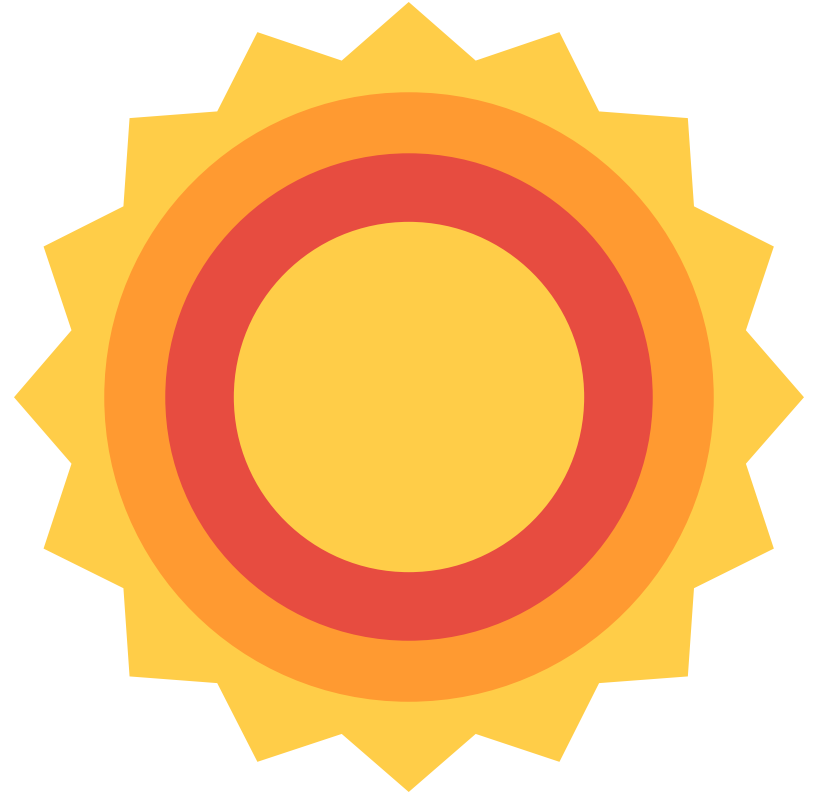
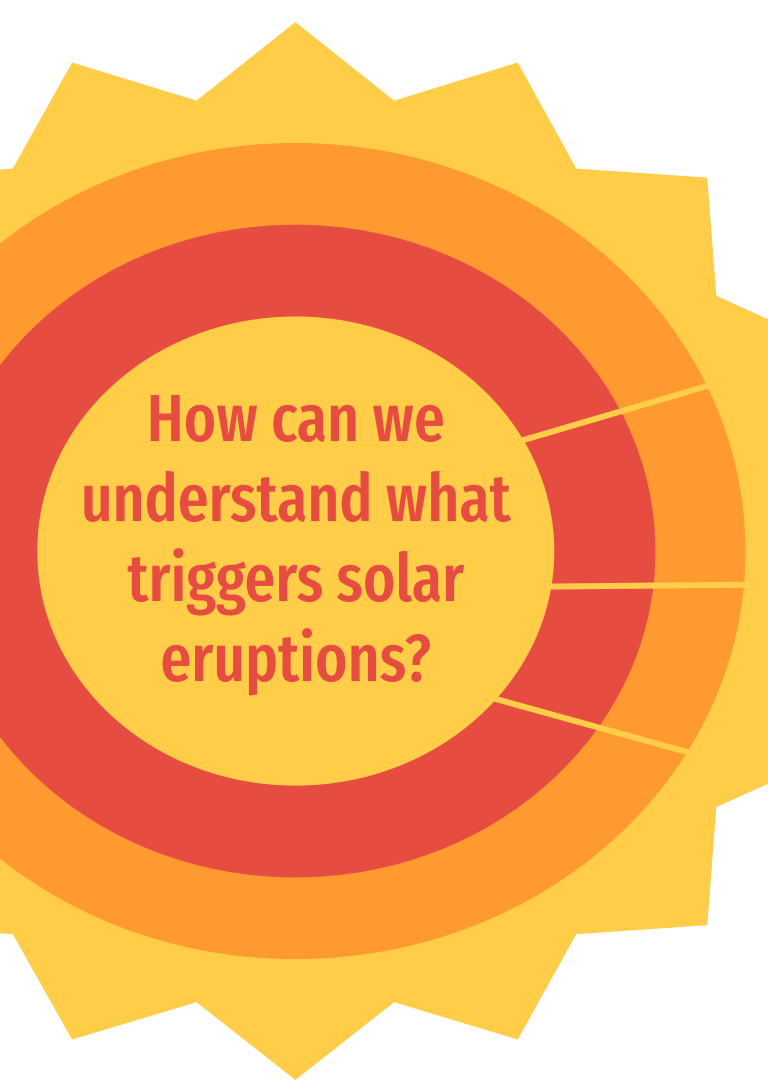


Investigation of Early Bursts during Flare Precursor

Zoe Schlossnagle & Dr. Chunming Zhu





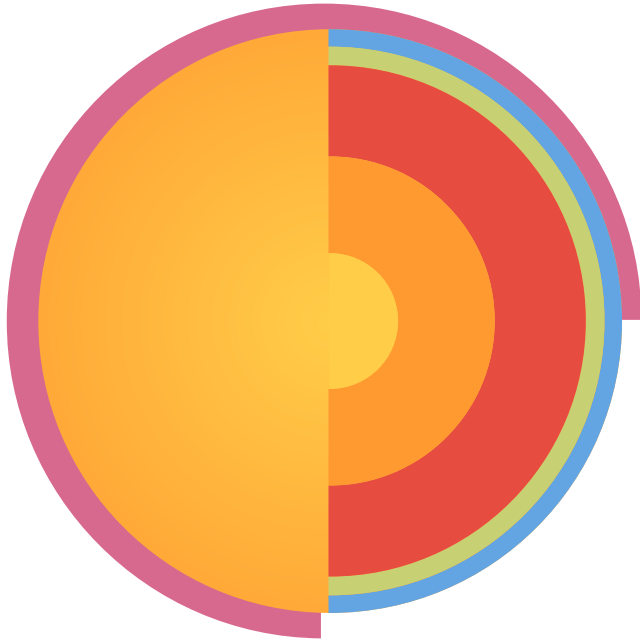
Motivation

Analyze data from NASA's SDO satellite

Find and characterize early signatures

Categorize events and compare with models

Procedure



1. Got familiar with IDL and the Sun's triggering mechanisms

2. Began mapping areas of interest on the Sun

3. Identifying flaring pixels

4. Stats for the three flares based on reconnection rate

5. Magnetic field extrapolation and geometry

Three Categories

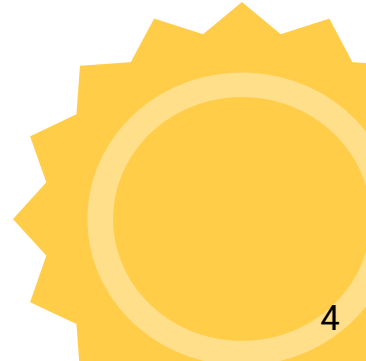
Events	Flare class	SDOxy	t ₀ (bursts)	t ₀ (CME)	FE?	Category
20100801	C3.2	[-480, 190]	06:41	07:34		1
20100807	M1.0	[-530, 170]	17:55	17:57	Y	3
20110621	C7.8	[100, 240]	01:30	02:09		2
20110802	M1.5	[240, 160]	04:26	05:50	N	1
20111001	M1.3	[90, 50]	08:57	09:35	Y	1
20111109	M1.2	[-500, 320]	12:32	12:56	Y	2
20120119	M3.2	[-350, 600]	13:42	14:17	Y	3
20120123	M8.8	[300, 580]	00:33	03:33	Y	1
20120309	M6.4	[50, 400]	03:21	03:21	N	1
20120310	M8.5	[350, 400]	17:19	17:14		1
20120405	C1.6	[480, 370]	20:12	20:09	Y	3
20120508	C1.7	[50, 300]	09:30	09:21	N	3
20120614	M1.9	[-100,-300]	12:33	13:04	N	2
20120712	X1.4	[20,-300]	14:21	16:08	N	3
20120927	C3.8	[490, 80]	23:35	23:20	Y	3
20121023	C2.9	[380, 180]	07:39	07:44	N	3
20131207	M1.3	[720,-250]	07:16	07:09	Y	3

Zhu et al. (2022, AGU)

Category 1: Early brightening occurs inside the ribbons

Category 2: Early brightening occurs outside the ribbons

Category 3: Early brightening does not occur

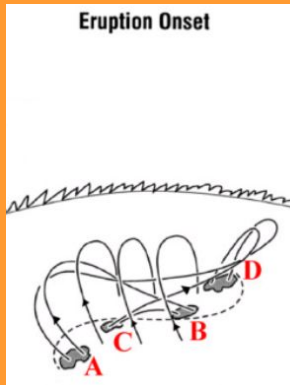


Triggering Mechanisms (*Forbes 2000; Chen 2011*)

Tether Cutting

1

Early brightening occurs **inside** the flare ribbons

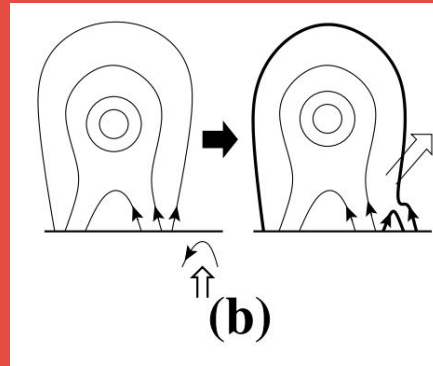


Moore, et al 2001

Flux Emergence

2

Early brightening occurs **outside** the flare ribbons

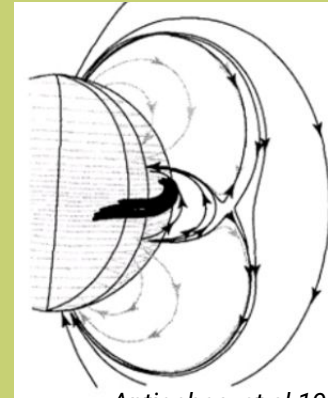


Chen 2008

Breakout Model

2

Early brightening occurs **outside** the flare ribbons



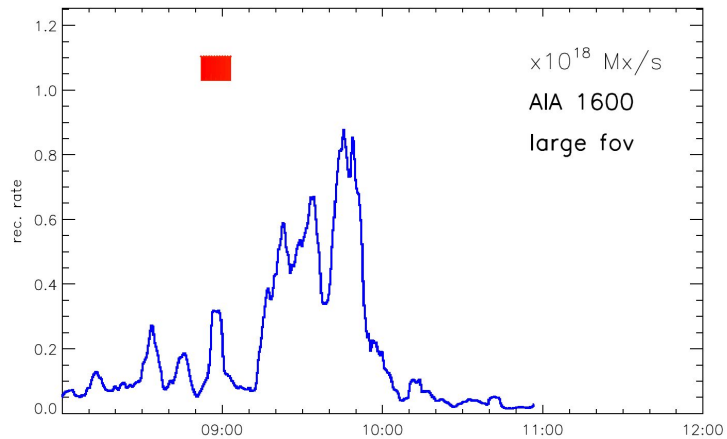
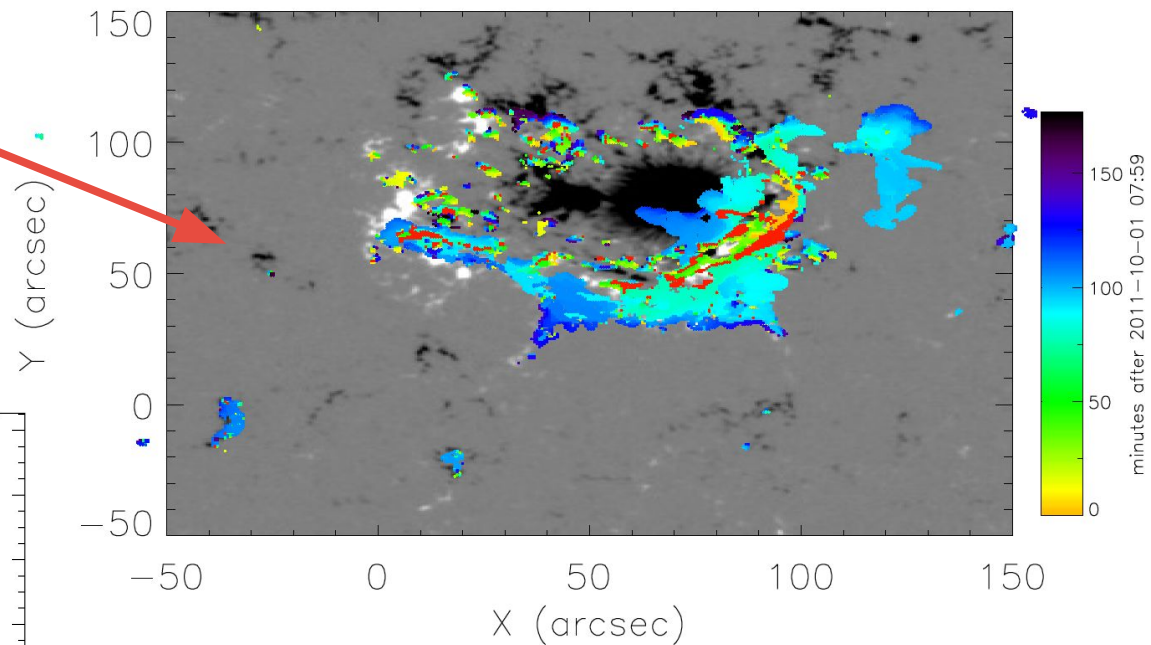
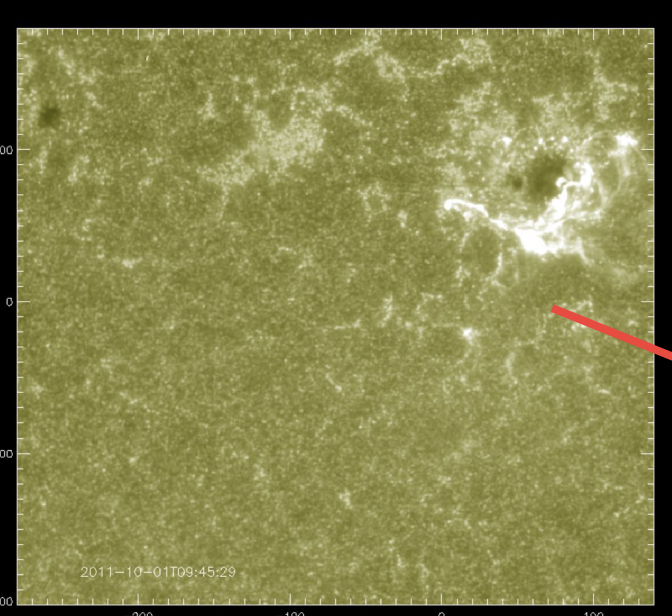
Antiochos, et al 1999

Instability

3

Ideally, no Early brightening

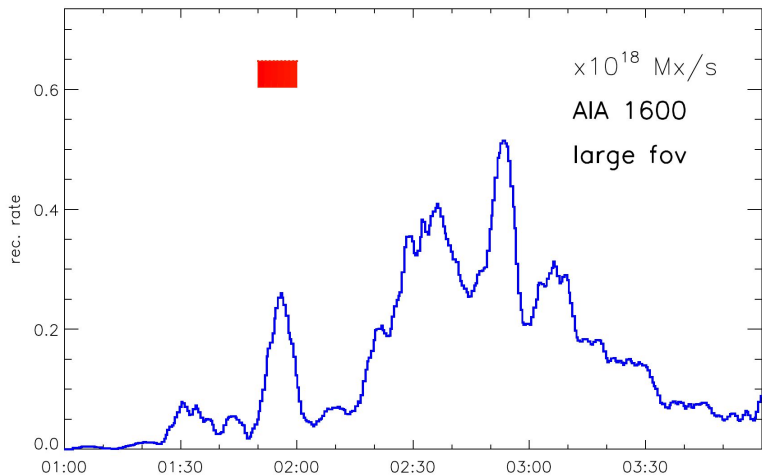
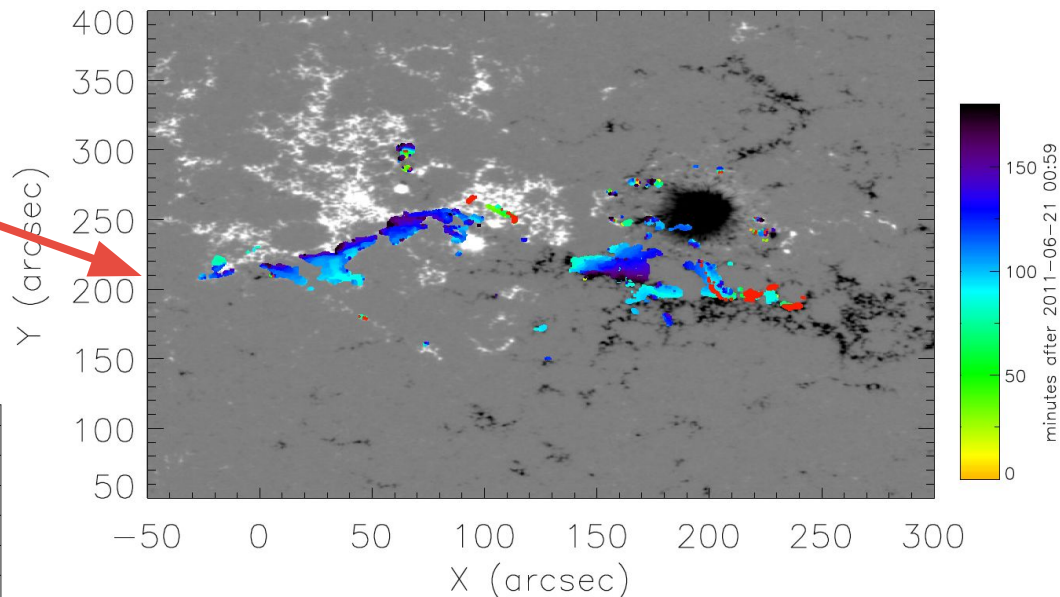
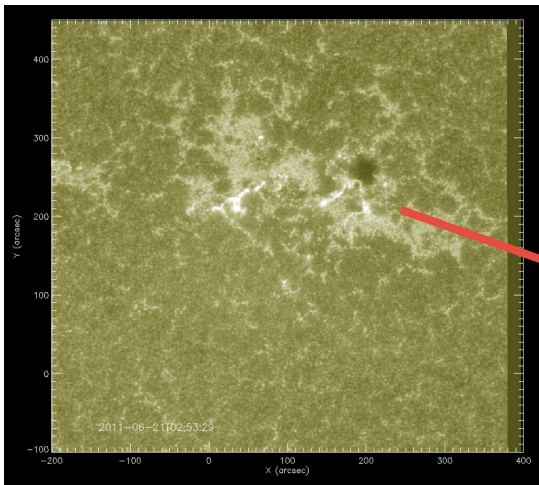
Mapping flaring pixels: Category 1



October 1, 2011 event shown in AIA 1600 (left) and as an over-layed magnetogram (right)

Measuring Method see Qiu et al. (2002)

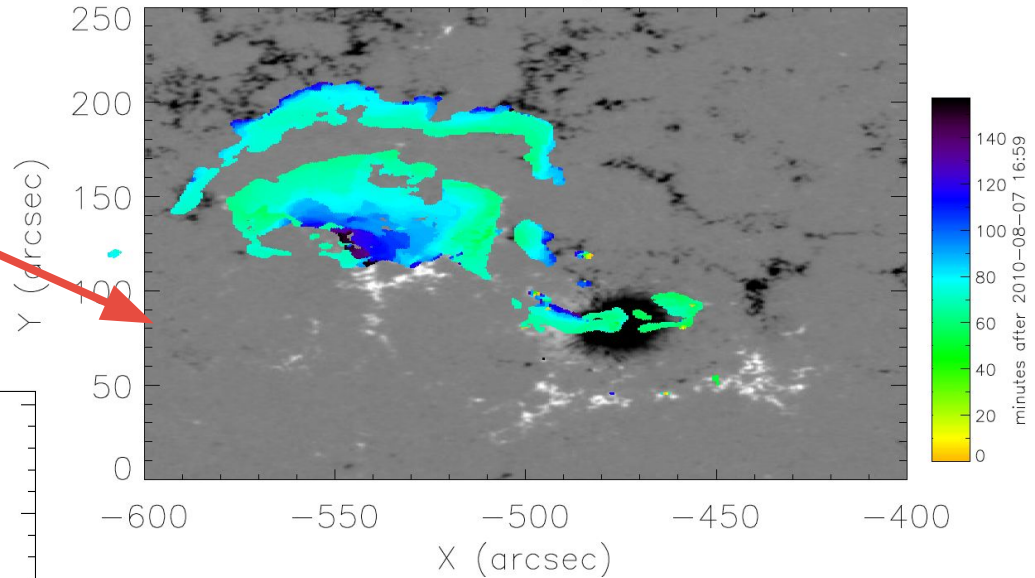
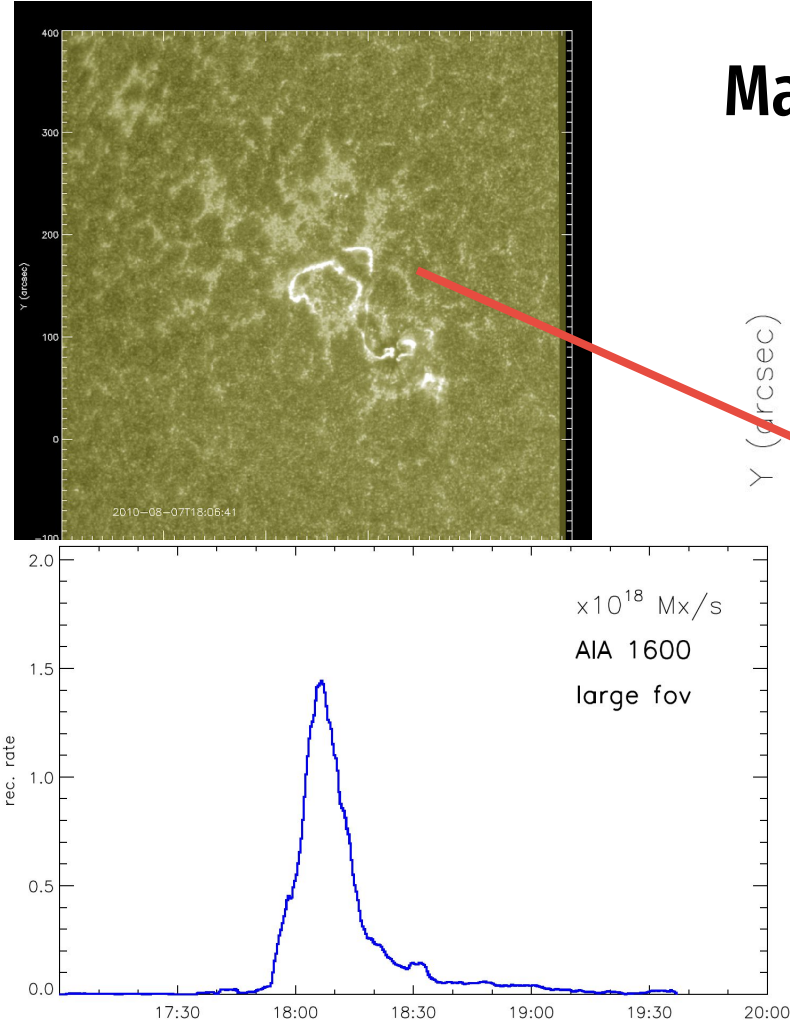
Mapping flaring pixels: Category 2



June 21, 2011 event shown in AIA 1600 (left) and as an overlaid magnetogram (right)

Measuring Method see Qiu et al. (2002)

Mapping flaring pixels: Category 3



August 7, 2010 event shown in AIA 1600 (left) and as an over-layed magnetogram (right)

Measuring Method see Qiu et al. (2002)

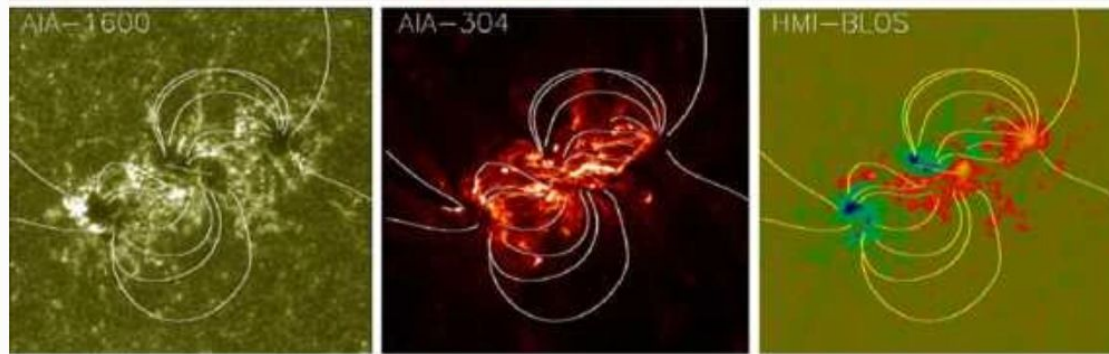
How do they compare?

		20111001 (Cat. 1)	20110621 (Cat. 2)	20100807 (Cat. 3)
Duration (min)	Burst	4:34	7:22	0:00
	<i>Flare</i>	31:41	42:59	11:50
	Ratio	0.144	0.171	0
Pk Reconn. Rate (10^{18} Mx/s)	Burst	0.31784	0.260236	0
	<i>Flare</i>	0.877078	0.514297	1.44278
	Ratio	0.362	0.506	0
Time btwn starts (min)		25:09	34:56	0

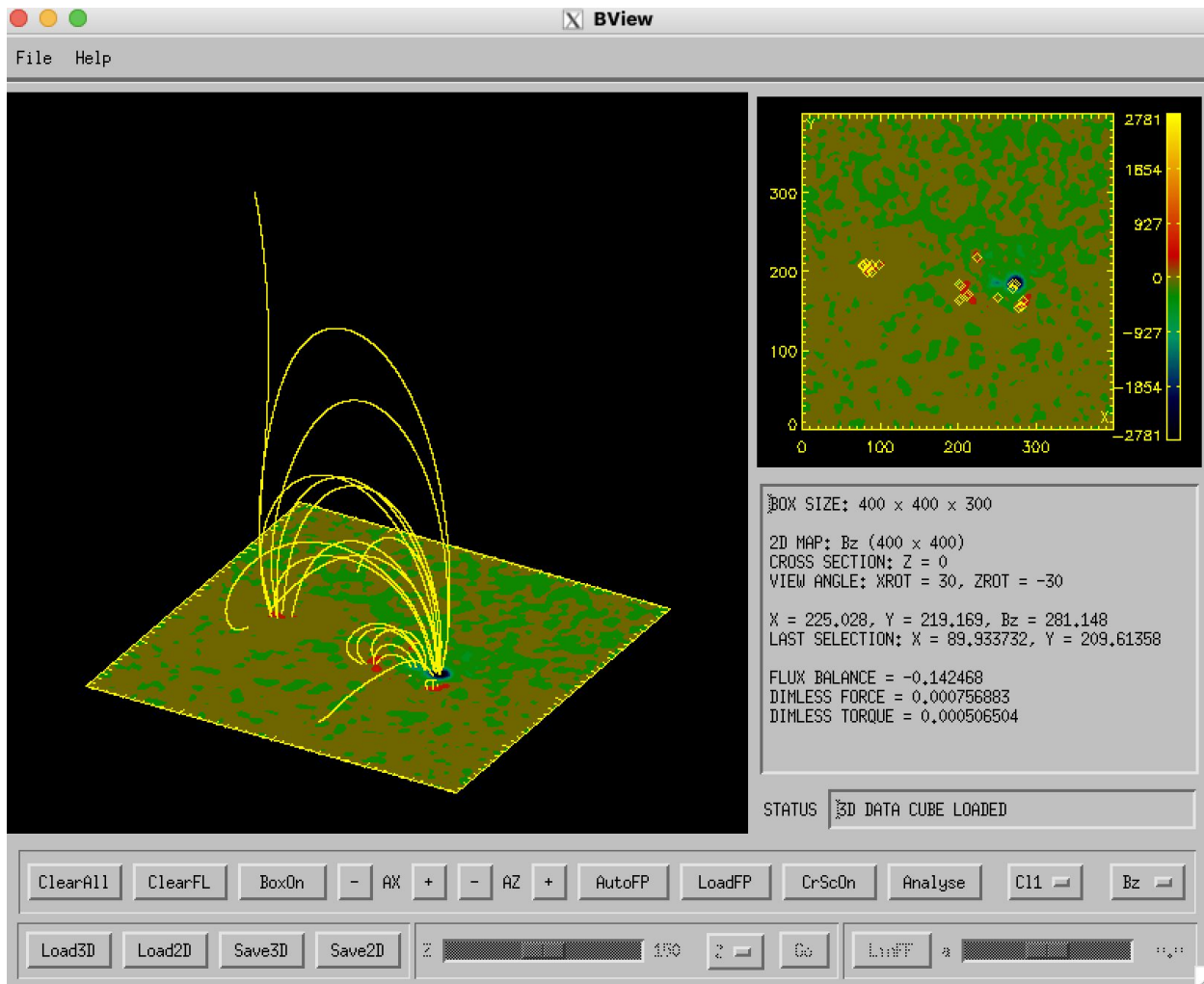
Magnetic Field Extrapolation

GOAL: reconstruct and model the magnetic field above an active region of the Sun for non-linear and force-free fields (NLFFF)

$$(\nabla \times \mathbf{B}) = \alpha \mathbf{B}$$



(Wiegmann et al. 2012)

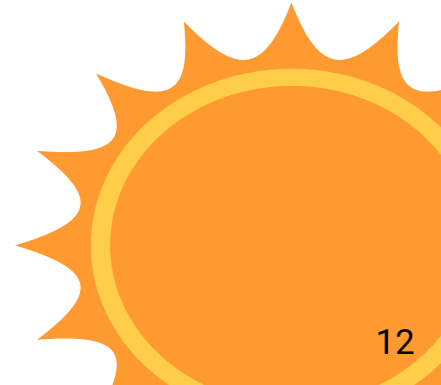


Magnetic field extrapolation results for the October 1, 2011 event

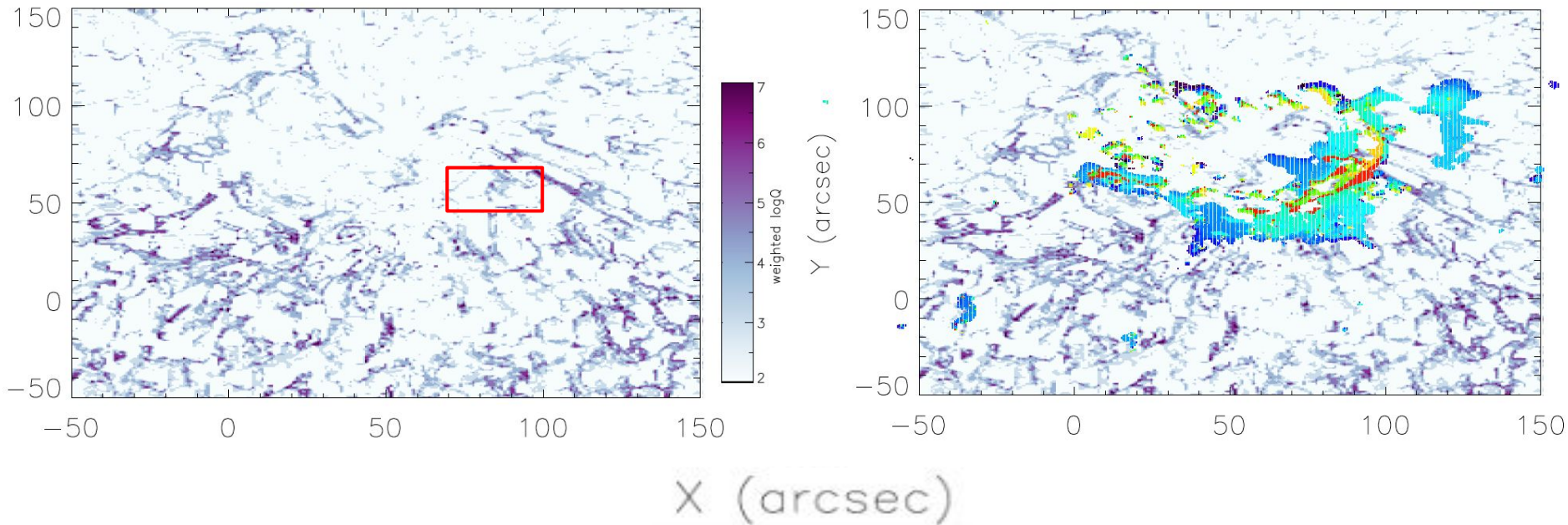
Squashing Factor Q

Q is used to quantify the stretching and squashing of magnetic field lines
(Titov et al. 2002, 2007; Longcope 2005; Liu et al. 2016)

A way to show field connectivity and geometry

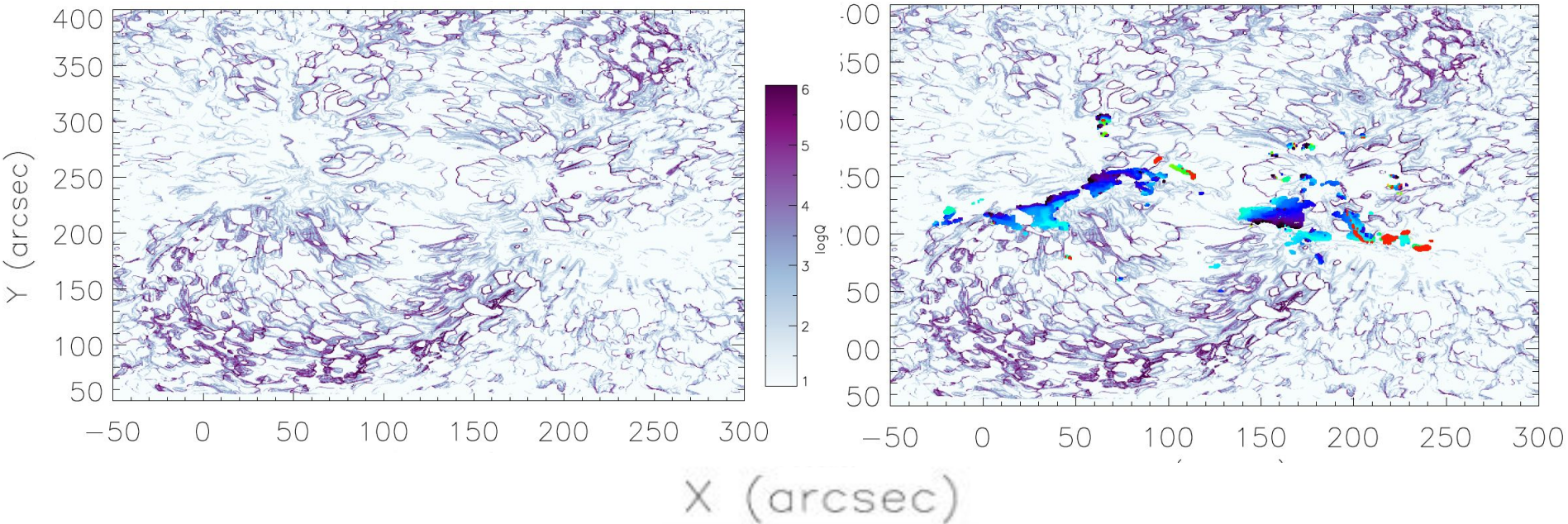


Q-factor and flaring pixels over time 10/01/2011 (1)



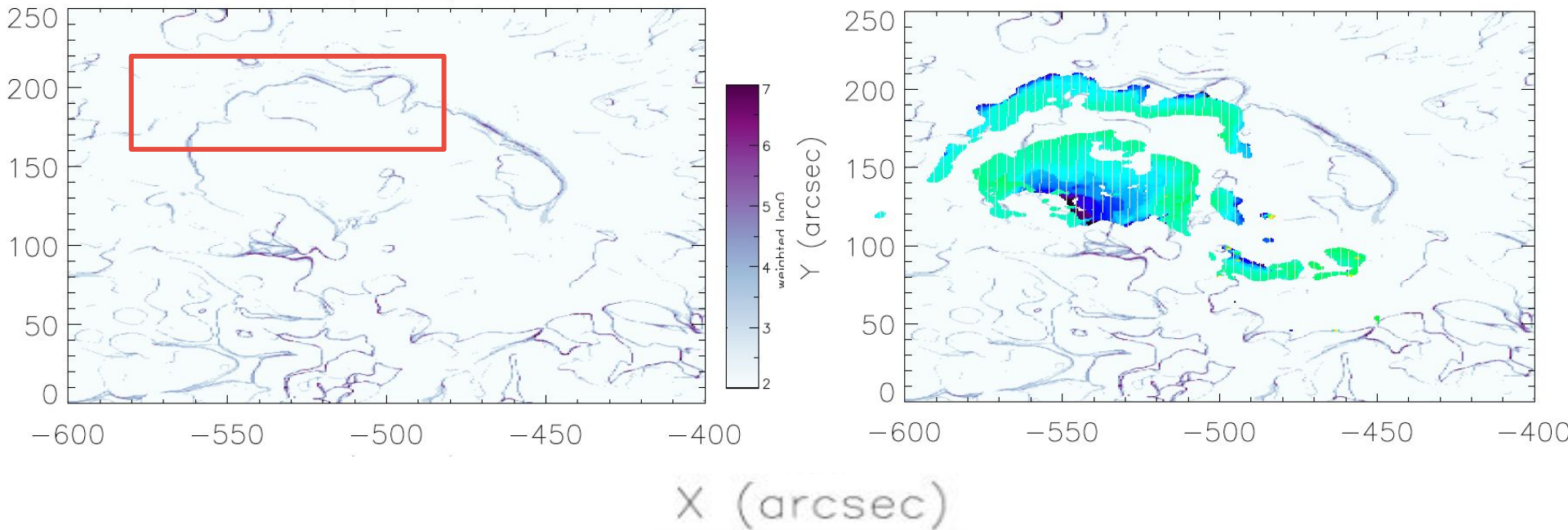
Q-factor and flaring pixels over time

06/21/2011 (2)

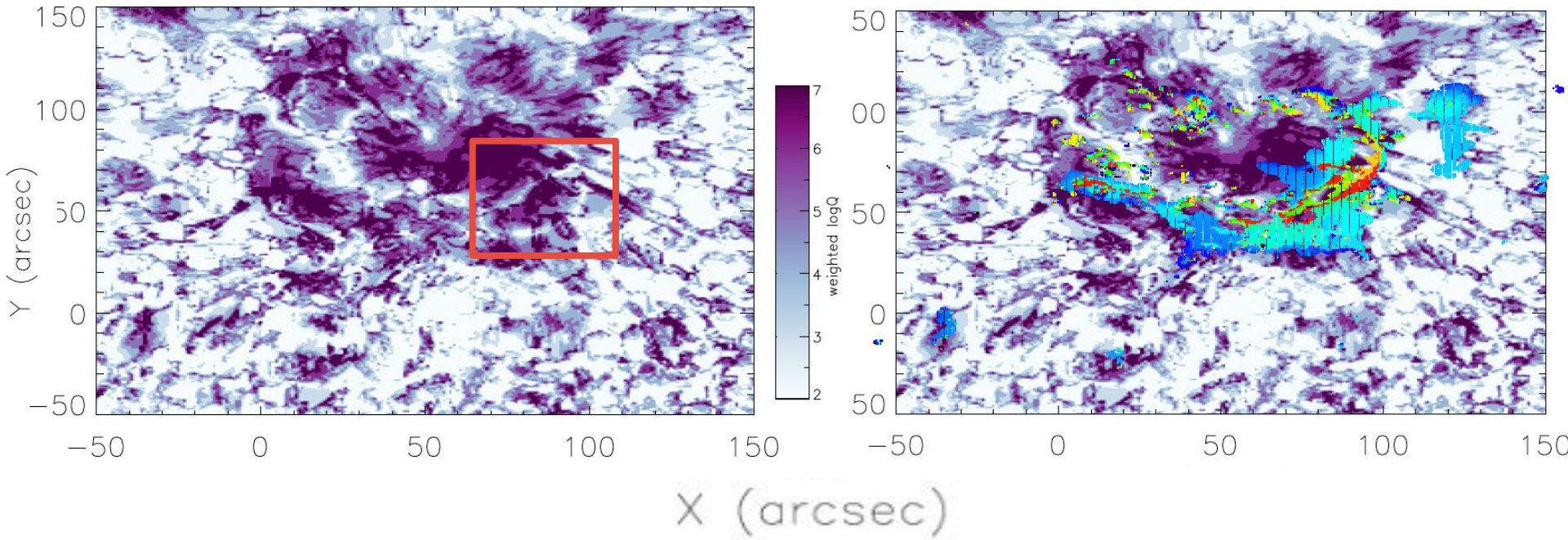


Q-factor of flaring pixels over time

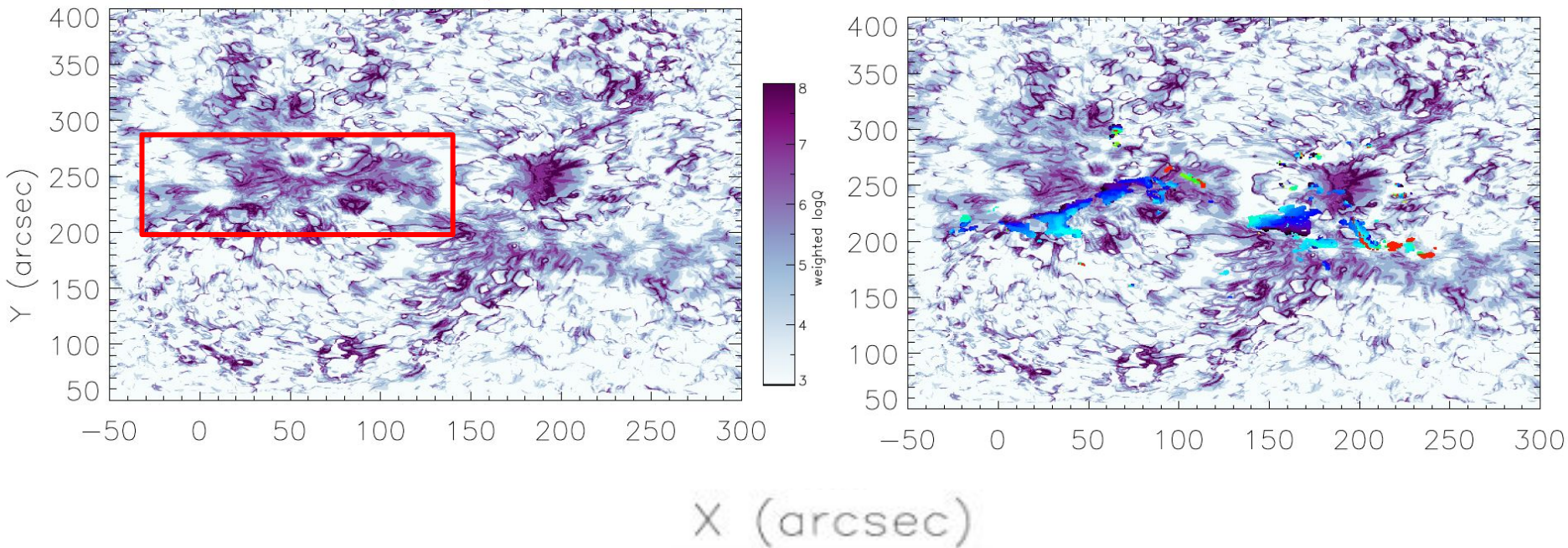
08/07/2010 (3)



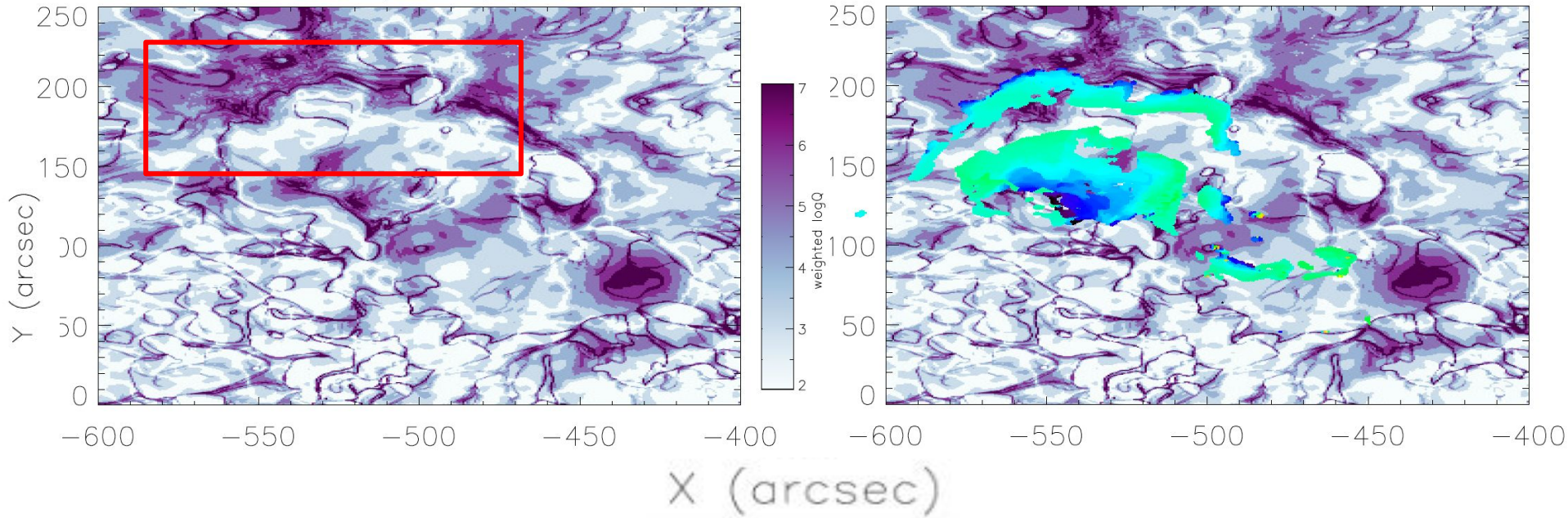
Bz² Weighted Q: 10/01/2011



Bz^2 weighted Q: 06/21/2011



Bz^2 weighted Q 08/07/2010



Summary

We investigate the characteristics of early bursts during the precursor phase of flares, to understand what role magnetic reconnection plays in the initiation of solar eruptions. By now, we have studied 3 out of 17 flares, with one in each of the three categories.

[1] Stats: duration, reconnection rate of magnetic flux (compared with major flare)

[2] Evaluated the magnetic field geometry with field extrapolation and squashing factor Q

[3] Tested weighting method for Q map

In the following work, we will study further different weighting methods of the Q map (e.g., electric current), and extend the statistics and field geometry to all the 17 flares in our sample.

THANKS!

Chen, P.F. Coronal Mass Ejections: Models and Their Observational Basis. *Living Rev. Sol. Phys.* 8, 1 (2011).
<https://doi.org/10.12942/lrsp-2011-1>

Forbes, T. G, A Review on the Genesis of Coronal Mass Ejections. *Journal of Geophysical Research: Space Physics*,
vol. 105, no. a10, 2000, pp. 23153-23165. <https://doi.org/10.1029/2000JA000005>.

Liu et al. 2016 Structure, stability, and evolution of magnetic flux ropes from the perspective of magnetic twist *ApJ* 818 148

Longcope, Topological methods for the analysis of solar magnetic fields. *Living Reviews in Solar Physics* 2.1 (2005): 1-72.

Qiu et al. 2002 Motion of Flare Footpoint Emission and Inferred Electric Field in Reconnecting Current Sheets *ApJ* 565 1335

Titov et al. 2007, Generalized Squashing Factors for Covariant Description of Magnetic Connectivity in the Solar Corona *ApJ* 660 863

Wiegmann, T., et al. How should one optimize nonlinear force-free coronal magnetic field extrapolations from SDO/HMI vector magnetograms?. *Solar Physics* 281 (2012): 37-51.

Zhu, C. et al. Early Bursts during Flare Precursor and the Relationship to Onset of Solar Eruption, AGU Fall Meeting, 2022